Dynamic Mechanical Analysis during polyurethane foaming: relationship between modulus build-up and reaction kinetics

Paula Cimavilla-Román[a]*, Mercedes Santiago-Calvo[a], Miguel Ángel Rodríguez-Pérez[a,b]

[a] Cellular Materials Laboratory (CellMat), Condensed Matter Physics Department, University of Valladolid, Paseo Belen 7, Valladolid 47011, Spain

[b] BioEcoUva. Research Institute on Bioeconomy, University of Valladolid

* Correspondence: Paula Cimavilla Román (E-mail: paulacimavilla@fmc.uva.es)

Abstract

The modulus build-up and relative density evolution during the reactive foaming of four standard polyurethane formulations was monitored in-situ by Dynamic Mechanical Analysis (DMA) with a customised set-up in parallel plate geometry. The modulus increased from 0.01 MPa in the first minutes to over 1.2 MPa within 20 minutes. The set-up also enabled the recording of vitrification followed by curing times. These typically occur within 3 minutes of each other. The results of DMA are corroborated by measurements of the reaction kinetics with Infrared Spectroscopy. This goes to show that the modulus remains nearly unchanged during the stage of swiftest isocyanate conversion, while the point of gel conversion is accompanied by their increase.

Keywords

Dynamic Mechanical Analysis; Rheokinetics; FTIR Spectroscopy; Rigid Polyurethane foams; Chemical reactions.

1 Introduction

By the end of 2019, polyurethane (PU) products represented more than 9% of the European plastic consumption [1]. Unlike other polymers, PU encompasses a wide variety of materials ranging from thermosets adhesives to thermoplastic elastomers and foam products. The versatility of this polymer is the main reason accounting for its extensive consumption. Among these PU-based materials, foams represent around 67% of their global consumption [2]. There are two main types of PU foams.

On the one hand, flexible foams are mainly used in comfort applications and transportation due to their load-bearing capacity and resilience [3]. On the other hand, due to its low thermal conductivity and excellent mechanical properties, rigid polyurethane foams (RPU) are used in a myriad of applications, such as insulating materials for construction, insulators for refrigeration systems as well as structural elements in the automotive industry [4–6]. Modern society's demands and increasing pressure from governmental institutions require constant research on these materials to enhance properties, ensure their sustainability and expand their applicability limits [2,7–9].

Enhancing the properties of RPU foams' unavoidably involves modifying current formulations and production routes [10–15]. As a consequence of the complexity of the foaming process of these materials, fine-tuning formulations or changing the initial raw materials by a trial-and-error approach is an arduous task. Boosting these material's performance requires a deep understanding of the modifications undergone by the initial raw materials by the reaction. RPU foams are the result of two exothermic reactions, one between isocyanate with hydrogen active groups stemming from the polyol and another one between isocyanate and water. The reaction between isocyanate and polyol, *gelling reaction,* is responsible for generating urethane cross-links. While the reaction between isocyanate and water, known as *blowing reaction,* releases CO_2 gas and generates urea hard segments. The release of CO_2 at early stages of the reaction, when the polymer is still a low modulus and low molecular weight gel, leads to foam expansion. Prior to the foam expansion, the CO_2 gas generated saturates the reactive mixture. Once the amount of gas in the mixture exceeds the solubility limit, this thermodynamic instability leads to the nucleation of cells, which later grow due to the ongoing blowing reaction [16]. Cell growth progresses until the polymer matrix has reached a limiting stiffness from which the foam expansion can no longer continue.

Therefore, producing foams with optimum properties requires attaining a delicate balance between cell nucleation, cell growing, cellular structure stabilisation, fast polymerisation of the initial reactive mixture and a swift viscosity increase of the polymer matrix. Any additional components, such as catalysts, surfactants or fillers, drastically modify this balance [13,17,18]. Hence, it is vital to characterise the

equilibrium between the different phenomena and physical magnitudes that ultimately condition the final cellular structure, polymer morphology and foams' properties[17]. This is why there has been a rise in the number of *in-situ* techniques enabling researches to gain insight into the RPU foam formation in the last years [14,19–21].

These *in-situ* techniques can be divided into two groups depending on whether they follow the chemical or physical events leading to the foam formation. On the chemical side, infrared expandometry, foaming temperature measurements, FTIR spectroscopy, and small-angle X-ray scattering (SAXS) are well-established techniques that give information about the system's reactivity [13,19,22,23]. FTIR spectroscopy and SAXS provide information about the kinetics of both gelling and blowing reactions, and about the development of a microphase separated polymer morphology [13,19,22]. In addition, PU foaming is exothermic and the foaming temperature evolution can be monitored by inserting thermocouples into the material. [23]. Similarly, infrared expandometry allows probing the sample's surface temperature as well as the foam expansion [24]. On the physical side, imaging techniques and rheology have been used to understand the mechanisms of foam formation. On the one hand, X-ray Radioscopy and *in-situ* optical imaging have been used to observe cell growth and degeneration of the cellular structure [16,25]. On the other hand, previous studies have also shown that by employing shear rheology, it is possible to measure the evolution of the foam's modulus with time [20,26,27]. Using a rheometer with a flooded parallel plate geometry, Mora et al. [26] studied the evolution of flexible PU foams' shear modulus with time. During the reactive foaming process, the authors were able to identify four phenomenological stages, corresponding to bubble nucleation, liquid foam, phase separation and a final stage corresponding to the already foamed material.

Despite the success of rheology in measuring the foam's modulus development and identifying the different foam formation stages, this technique is not as widespread as the previously mentioned *in-situ* techniques. The reason lies in the relative complexity of the method, a reputation for mathematical complexity, and the technical difficulty of keeping the growing foam between the equipment plates [28]. The latter necessitates a small gap between the parallel plates, which limits the

sample's mass to a low value. Thus, only foams of a few layers of cells in thickness can be investigated [29]. In order to avoid this, there are reports of flooded parallel-plate geometries with which larger samples can be accommodated [26]. The trade-off is the variation of the foam's mass between the plates during the experiment, which limits the accuracy of the experimental results.

Another common technique for the determination of the viscoelastic properties of polymers is Dynamic Mechanical Analysis (DMA). DMA provides information on major and minor transitions of solid polymers and it has been used extensively to measure the mechanical properties of viscoelastic materials as a function of temperature or frequency [28]. In addition, DMA has been also employed to measure the curing process of thermosets [28]. However, the technique has never been applied to investigate the simultaneous polymerisation and growth of polyurethane foams. This absence of reports on the application of DMA during the foaming process of thermosets could be explained by the disparate transformations undergone by solids and foams during polymerisation. In fact, non-foaming polymers during cure experience a minimum volume change which pales in comparison to that suffered by a foaming thermoset; for instance some PU foams experience a volume increase superior to thirty times [24,30]. Therefore, the existing methods to measure the modulus of curing thermosets cannot be directly translated to materials undergoing a simultaneous foaming process. Nonetheless, employing a customised fixture, like the one reported in this work, it is possible to keep the growing foam in contact with the measuring plate while maintaining the mass constant underneath it. This allows measuring the expansion ratio simultaneously to the modulus increase, which cannot be achieved with rheometers [28]. In this study, we propose a simple methodology based on DMA to measure the modulus development of RPU foams for the first time. To establish the method and determine its accuracy, we investigated four conventional RPU formulations with varying blowing agent (water) and catalyst content. The approach proposed here can deepen the understanding of the foaming process of PU systems, and the results obtained, modulus and viscosity increase vs time, could be implemented in existing models for the growing stage of RPU foams.

2 Experimental

2.1 Materials

2.1.1 Reactants of RPU foams

The polyol component was a high functionality polyether polyol, Alcupol R4520 (4.5 functionality, OH value of 455 mg·KOH/g, viscosity 5250 mPa·s) from Repsol S.A. The isocyanate was a polymeric diphenylmethane diisocyanate (pMDI), IsoPMDI 92140 (2.7 functionality, 31.5% NCO, density 1.23 g cm^{-3}, viscosity 170-250 mPas) supplied by BASF. TEGOAMIN® DMCHA (N,N-dimethylcyclohexylamine) from Evonik was employed as a catalyst, a tertiary amine used primarily to promote urethane (polyol-isocyanate) reaction. TEGOSTAB® B8522 (a non-hydrolysable polyether-polydimethyl-siloxane–stabiliser) from Evonik was used as a surfactant to obtain superior cell structures. Distilled water was chosen as a blowing agent.

2.1.2 Preparation of RPU foams

Four different RPU foams were prepared, maintaining a constant isocyanate index. The formulations are presented in Table 1. While the polyol and surfactant contents were kept constant, the amount of catalyst (0.5 and 1.5 parts per weight (ppw)) and blowing agent (2 and 5 ppw) was changed independently.

The different components were mixed with an overhead stirrer (EUROSTAR 60 control from IKA), equipped with a 50 mm diameter VollrathTM Lenart-disc. A homogeneous polyol blend with the additives (catalyst, surfactant and blowing agent) was produced at 250 rpm for 2 minutes. To trigger the foaming reaction, a total mass of 40 g isocyanate and polyol blend was mixed during 10 s at 1200 rpm in a plastic cup. The start of the stirring process between polyol blend and isocyanate is set to time 0 of the reaction.

Table 1. RPU formulations.

Samples	Isocyanate Index	Polyol (ppw)	Surfactant (ppw)	Gelling catalyst (ppw)	Blowing agent (ppw)
REF	110	100	1	0.5	2
BAF	110	100	1	0.5	5
GCF	110	100	1	1.5	2
GBF	110	100	1	1.5	5

Following the formulations in Table 1, RPU foams with 40 g of material (large samples) were produced. Foams with low blowing agent content REF (Reference Formulation) and GCF (Gelling Catalyst Formulation) reached foam volumes of *ca.* 750 cm^3. In contrast, foams with high blowing agent content, BAF (Blowing Agent Formulation) and GBF (Gelling Blowing Formulation) attained foam volumes of nearly 1200 cm^3. These foams were left to cure at room temperature for one week. After this period the foams were cut, and the final density was characterised. DMA experiments were carried out to obtain stress-strain curves and the complex modulus of the cured foams.

In addition, around 100 mg from the reactive mixture were extracted from the plastic cup just after the stirring process to study the viscoelastic properties by time-resolved DMA experiments, the reaction kinetics by time-resolved FTIR spectroscopy and the reactivity of the foams by measuring the characteristic times of foam formation (see next sections for a detailed explanation of these measurements).

2.2 Methods

2.2.1 Reactivity of the foams

The system's reactivity can be roughly estimated by measuring characteristic times of the RPU foam formation, *i.e.* cream time, string or gel time, rise time, and tack-free time [21]. These times were determined using samples of similar mass to those tested in DMA experiments (100 mg). The samples were kept inside a furnace at 50 °C during the testing.

2.2.2 Density characterisation of the foams

Foam density was measured as described by ASTM D1622/D1622M-14 [31]. Density was measured on three different samples for each material, with a diameter of 30 mm and a height of 20 mm. Relative density was obtained as the ratio between the foam density and the solid material density (1160 kg/m^3).

2.2.3 Dynamic Mechanical Analysis

Viscoelastic properties during the growing and curing of foams in Table 1 have been measured using a Perkin-Elmer DMA 7. The equipment was operated in

compression mode, employing a 10 mm-diameter parallel plate configuration where the upper plate is mobile and the lower plate is fixed. DMA's operating principle is based on supplying an oscillatory force to a sample and studying its response. This force causes a sinusoidal stress to the sample under study, $\sigma = \sigma_0 \sin(wt)$, which generates a strain wave, $\varepsilon = \varepsilon_0 \sin(wt + \delta)$ as a response. Depending on the material's viscous or elastic character, the strain wave will be shifted by a certain phase angle (δ). Provided that the material is purely elastic, the wave response will be in-phase with the applied oscillation ($\delta=0$). On the contrary, a purely viscous material will respond with an out-of-phase strain wave ($\delta=\pi/2$). Therefore, by measuring the amplitude and the phase of the response strain wave, it is possible to calculate the storage modulus, (E'), the loss modulus (E"), the complex modulus (E*) and loss tangent, or damping, ($\tan \delta$), as well as the equivalent viscosity values.

$$E' = \frac{\sigma_0}{\varepsilon_0} cos(\delta) \quad (1)$$

$$E'' = \frac{\sigma_0}{\varepsilon_0} sin(\delta) \quad (2)$$

$$E^* = E' + iE'' = \sqrt{(E')^2 + (E'')^2} \quad (3)$$

$$tan(\delta) = \frac{E''}{E'} \quad (4)$$

Although DMA is well established as a technique with which to investigate the properties of solids and their transitions [28], it is rarely applied to the study of fluids or low viscosity samples. For this, rotational rheometers are more often employed. Whereas fluids in a rotational rheometer can shear and glide because the applied force is parallel to the strain, in a DMA, the force is normal to the material. Usually, fluids subjected to normal stress will merely flow away from the compression plate, thereby providing meaningless information. Hence, to study the foam's rheological properties during the expansion process, it was necessary to develop a customised accessory (Fig. 1). The designed fixture enables to accommodate unreacted and growing foams, which experience a quick transition from a fluid of low viscosity to a high modulus solid material. The accessory comprises a 15 mm-internal diameter Teflon cup with a piston of the same diameter and material. The customised piston can glide with low friction inside the container

by the force of either the expanding foam or the compression plate (Fig. 1 component 6). This piston also ensures that no leakage of the growing foam occurs. Due to the limited dimensions of the measuring system, the maximum foam volume that the cup can hold is *ca.* 2.5 cm^3. In addition, the height of the foam can be recorded, and from it, the sample volume can be calculated. Using the value of the initial mass and this calculated volume, it is possible to measure the density and relative density as a function of time.

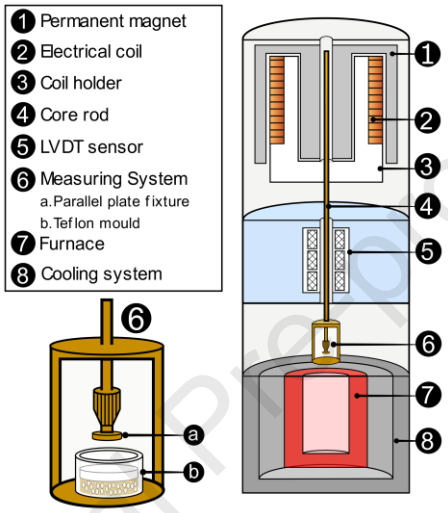

Fig. 1. Scheme of the main components in the DMA 7 analyser and the measuring set-up.

2.2.3.1 Experimental procedure of time-resolved DMA

The samples for the DMA tests were produced following the method detailed in Section 2.1.2. A few microliters were extracted from the cup containing the reactive mixture with a syringe and injected into the Teflon container (Fig. 1 component 6 b.). Simultaneously, the mass of the reactive mixture injected into the container was weighed using a precision balance. In order to ensure the reproducibility of the obtained results, the sample's mass was kept around 100 mg in all the experiments.

Once the sample was prepared, the piston was inserted into the cup, and the mould was placed in the measuring system (Fig. 1 component 6). The plate was lowered to record the initial height, after which the experiment began. The first experimental data point was recorded 2 minutes after the initiation of the reaction, meaning that the foam growth had already begun once the acquisition started. The experiment ended after 90 minutes since the start of the RPU foam reaction.

During these experiments, we chose to work under constant temperature (50 °C), constant frequency of oscillation (1 Hz) and controlled stress conditions. Data points were acquired every 6 s; thus, a total of 880 measurements were performed during the experiment. The sample was subjected to static stress of 509.3 Pa (static force: 90 mN) meant to hold the sample in place and to oscillatory or dynamic stress of 424.4 Pa (dynamic force: 75 mN) throughout the experiment. Under these conditions, the dynamic strain sinks from *ca.* 3%, when the mixture is soft, to *ca.* 0.05% at the end of the experiment. The low stresses applied were selected to obtain reliable values of the mechanical properties while still allowing the expansion of the foam.

An example of the technique's typical output when applied to investigate the foaming and curing process of an RPU foam can be seen in Section 3.3. Additionally, to ensure the method's reproducibility, at least three measurements were performed for every formulation.

2.2.3.2 DMA experiments of the cured foams

The mechanical properties of the foams produced ex-situ with 40 g of material (section 2.1.2) were also measured with DMA. The foams were cut into three sections; the central section had 20 mm of height and was extracted from mid-height of the foam. From the central section, at least two cylindrical samples of 13 mm of diameter were extracted, and all were investigated one week after their production. The experiment temperature and frequency were fixed at 50 °C and 1 Hz, respectively. The foams were subjected to a stress-strain test during which the dynamic stress increased linearly from 7.71 Pa to 7676.57 Pa. The static stress changed accordingly, and a ratio of 1.2 between the static and dynamic stress was kept constant for the entire run. In addition, to ensure comparability with the in-situ experiments, the complex modulus (E*) of the cured foams was calculated for the same values of force employed during the in-situ tests. [32].

2.2.4 Study of the reaction kinetics by FTIR Spectroscopy

Time-resolved FTIR spectroscopy is a common technique for monitoring the reaction kinetics of PU foams [13,27,33]. In order to validate the modulus build-up kinetics, FTIR spectra of the samples during foaming were collected using a Bruker

ALPHA spectrometer in attenuated total reflectance (ATR) mode. From the 40 g reacting mixture (section 2.1.2), 1 mL was extracted and poured onto the ATR cell's surface. The FTIR experiments lasted 90 minutes. A spectrum was acquired every 30 s - 180 spectra in total. The experiment's temperature was set to 50 °C, as it was for the DMA measurements. The isocyanate (NCO) consumption is extracted from the decrease in the area of the isocyanate band asymmetric stretching vibration at 2270 cm^{-1} [17]. To monitor the number of reaction products of the blowing and polymerisation reactions, the Amide I region (carbonyl region) located in the wavenumber range between 1610 and 1760 cm^{-1} was deconvoluted into 7 different bands encompassing all the urethane and urea compounds as indicated in the literature [13,34,35].

3 Results and Discussion

3.1 Reactivity of the foams

In order to evaluate the reactivity of the foams, the characteristic times of RPU foaming reaction were measured: cream time, string time, rise time and tack-free time. Firstly, cream time corresponds to the start of bubble nucleation, physically characterised by a change in the mixture's colour from a translucent dark brownish liquid to one cream-like. Secondly, the string time is the time at which the foam starts to polymerise or gel. It can be recognised by the thin strands or strings that can be pulled out of the foam when touching its surface with a sharp object. Thirdly, the rise time is the time at which the foam reaches its maximum expansion. Lastly, tack-free time is the time when the foam's surface loses its tackiness. It can be taken as the surface cure time of RPU foams. The characteristic times for the four RPU foams can be found in Table 2. On the one hand, REF and BAF foams were obtained using the same amount of gelling catalyst in the PU formulation (0.5 ppw), lower than that used in foams GCF and GBF (1.5 ppw). And since the gelling catalyst promotes the PU reactions, it can be observed that the characteristic times of the two latter materials are shortened. On the other hand, when RPU foams with the same amount of gelling catalyst and different water amount are compared (REF versus BAF, and GCF versus GBF), those materials with higher amounts of water in the PU formulation (BAF and GBF) reveal slightly lower characteristic times. On the

whole, the addition of water and catalyst promotes the system's reactivity, shortening the reaction times in line with expectations.

Table 2. Characteristic times of the RPU foams.

Samples	Catalyst (ppw)	Water (ppw)	Cream time (min)	String time (min)	Rise time (min)	Tack-free time (min)
REF	0.5	2	1.2 ± 0.1	4.2 ± 0.6	5.7 ± 0.9	14.9 ± 2.0
BAF	0.5	5	0.9 ± 0.1	3.7 ± 0.9	4.3 ± 0.2	15.6 ± 1.2
GCF	1.5	2	0.7 ± 0.02	2.0 ± 0.3	2.7 ± 0.3	6.7 ± 1.4
GBF	1.5	5	0.4 ± 0.7	1.4 ± 0.2	1.7 ± 0.1	5.7 ± 0.5

3.2 Foam density characterisation

In order to verify the evolution of the foam density detected during the DMA tests, the final geometric density of the foams produced with 40 g of material was measured (Section 2.1.2). Table 3 shows that the Reference foam (REF) with the lowest catalyst and water content (0.5 ppw and 2 ppw, respectively) has the highest density, followed by the foam produced with 1.5 ppw of gelling catalyst and 2 ppw of water (GCF). In contrast, the foams with 5 ppw of water (BAF and GBF) show the highest foam density decrease with respect to REF and GCF. Moreover, the lowest density was achieved for the foam with the highest water and catalyst content (GBF), which also presents the swiftest reaction kinetics according to Table 2. Therefore, the density is mainly determined by the amount of blowing agent and catalyst. A greater amount of water and gelling catalyst in the PU formulation gives rise to foams with lower densities.

Table 3: Density and relative density of the foams produced following Section 2.1.2

Samples	Catalyst (ppw)	Water (ppw)	Density (kg/m^3)	Relative Density
REF	0.5	2	60.4 ± 1.1	0.052
BAF	0.5	5	37.7 ± 1.1	0.033
GCF	1.5	2	59.5 ± 3.7	0.051
GBF	1.5	5	33.1 ± 1.6	0.029

3.3 Foaming and curing kinetics: Time-resolved DMA

Fig. 2 illustrates the main results obtained from a single DMA experiment for the formulation with a low concentration of blowing agent and catalyst (REF). From these data, the different chemical and physical events that lead to changes in the

sample's viscoelastic properties can be identified [20,26,27,36]. Firstly, it can be appreciated how the sample's modulus remained rather low and unchanged during the foam expansion (at times lower than 10 min). However, due to the relatively long loading time, the sample's porosity was already high when the run started. In fact, relative density was below 0.63 at the beginning of the experiment, and this value decreased to a final relative density of 0.1 in less than five minutes. Because of the low modulus values, it can be concluded that the mixture was still a low-molecular-weight gel that expanded due to the force of the CO_2 gas being generated during this stage. The second stage, at times longer than the string time (Table 2), was accompanied by the rapid build-up of both moduli. This increase was due to the stiffening of the polymer matrix by the generation of a stable cross-linking network [37]. In this stage, the loss modulus progressed to a maximum that several authors have previously ascribed to the Berghams or vitrification point [25,38,39]. From a thermokinetic point of view, vitrification is reached when the reactive mixture's glass transition temperature becomes equal to the curing temperature [40]. At vitrification, the morphology freezes, decreasing the chain mobility and hence reducing the curing rate. From this point on, the reaction becomes diffusion-controlled [41]. Finally, once the reactivity of the system had quenched, the polymerisation speed decreased, and the storage modulus reached a plateau region. After this, the moduli continued to grow. Although the speed of increase is reduced considerably, and the remaining changes in moduli result from the long reactivity of RPU foams, which continue to cure long after the reaction starts. In addition, for this specific formulation, the storage modulus attained nearly 75% of its final value after 20 minutes from the reaction start.

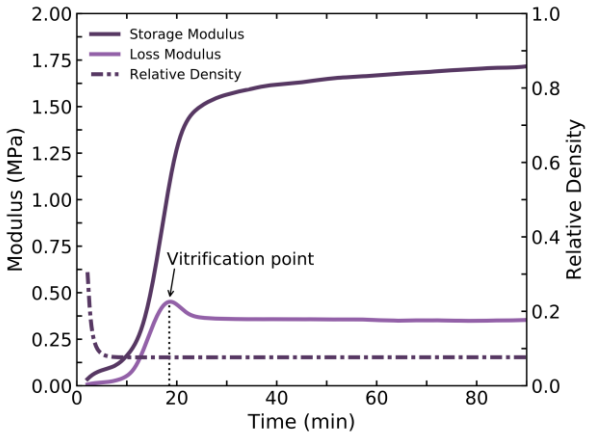

Fig. 2: Example of the results obtained during a typical DMA experiment for sample REF (0.5 ppw catalyst and 2 ppw water)

All the formulations in Table 1 were studied according to the same experimental procedure detailed in Section 2.2.3.1. Fig. 3 represents the average values and the standard deviation of the storage and loss modulus after repeating the measurements three times for different samples produced with the same formulation. As can be seen, the standard deviation is considerable, yet the differences between the foams are clear, and it is possible to distinguish not only the final foam's modulus but most notably the reaction speeds.

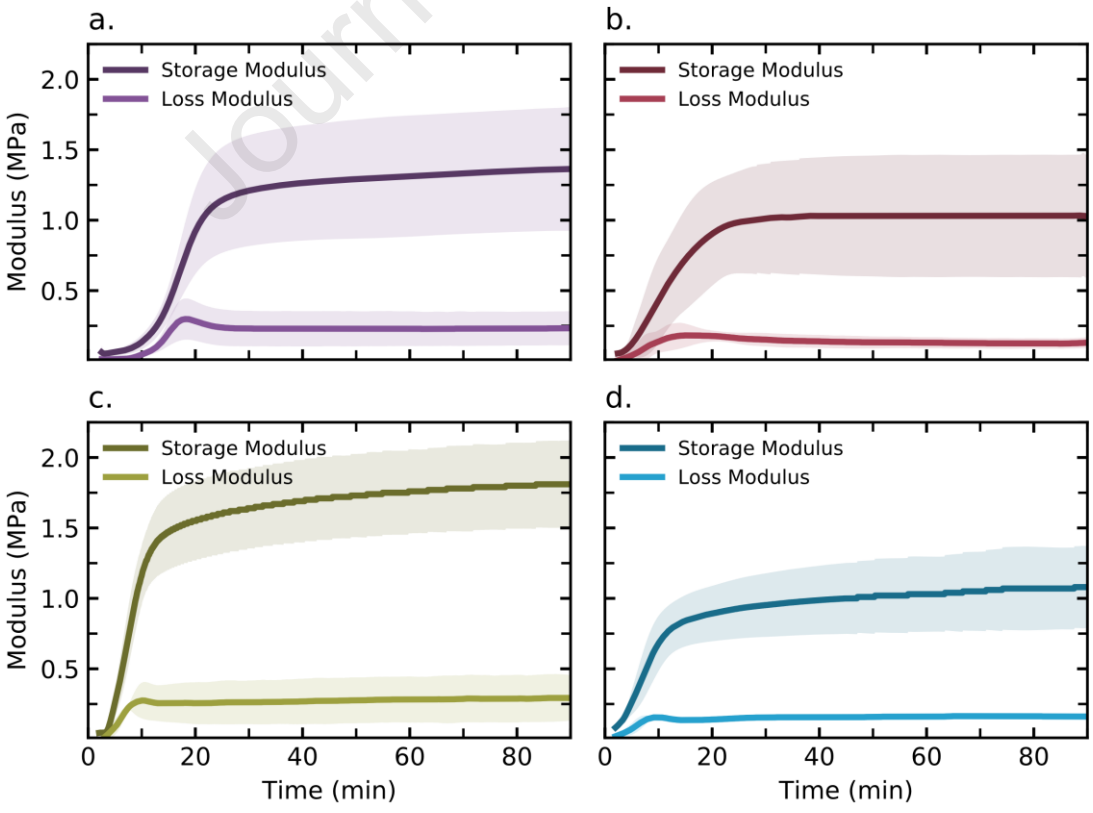

Fig. 3. Moduli development as a function of time for each of the foams in Table 1 a. REF (0.5 ppw catalyst and 2 ppw water), b. BAF (0.5 ppw catalyst and 5 ppw water), c. GCF (1.5 ppw catalyst and 2 ppw water), and d. GBF (1.5 ppw catalyst and 5 ppw water).

It can be observed how the onset of the storage modulus build-up and the time at which the foams' modulus stabilised was longer for the formulations with the least catalyst content (Fig 3. a and b). In fact, foams REF (Fig. 3 a.) and BAF (Fig. 3 b.) took more than 30 minutes to reach the storage modulus plateau. In contrast, formulations with the highest catalyst dosage (Fig 3. c and d) show the opposite trend. An almost immediate modulus development is appreciable as soon as the experiment starts. This is followed by a quick modulus build-up. Apart from this, the relative density decrease was also faster for the foams with more catalyst (Fig. 4), an observation that is in good agreement with the rise times reported in Table 2. Lastly, information can also be extracted from the slope of the storage modulus increase: foams with higher blowing agent content (Fig 3. b and d) revealed a slower transition from a low modulus gel to a cross-linked solid. Particularly, BAF (Fig. 3 b.) and GBF (Fig. 3 d.) presented slopes of 0.063 and 0.083 MPa/min, respectively, whereas foams REF (Fig. 3 a.) and GCF (Fig. 3 c.) reached much higher speeds of modulus increase in the region of 0.099 and 0.190 MPa/min, respectively. Therefore, on average, formulations with less water exhibited twice the speed of elastic modulus increment.

As alluded to previously, the loss modulus also provides some information regarding each foam's curing and polymerisation kinetics. Most importantly, the vitrification time is observed to decline with decreasing catalyst content (Table 4). This implies that the samples with weaker catalysis take longer to achieve the glassy state characteristic of amorphous thermosetting PU and thus to reach the glass transition temperature of the final material [42]. It can be surmised that vitrification stands for a form of curing time at which the polymer reaches the high stiffness characteristic of RPU foams. This rationale is in agreement with the curing kinetics that can be inferred from the storage modulus evolution. In fact, it is observed that shortly after the vitrification time, the foams attained nearly 75% of their final modulus in the time-resolved DMA experiments (Table 4). However, due to the long loading times and the lower precision of DMA when the foam is in a fluid state, it was not possible to identify the gelation time, which in principle should be at the crossover between the storage and loss modulus [26,42,43].

Table 4. Vitrification times (extracted from the average loss modulus in Fig. 3) and time at which the storage modulus had progressed to 75% of the final value.

Samples	Catalyst (ppw)	Water (ppw)	Vitrification time (min)	75% of cure time (min)
REF	0.5	2	18.6 ± 1.1	21.5 ± 1.9
BAF	0.5	5	15.3 ± 1.9	15.9 ± 2.6
GCF	1.5	2	9.4 ± 1.3	10.6 ± 1.6
GBF	1.5	5	9.3 ± 1.1	13.1 ± 3.7

Furthermore, the DMA measurements also mapped the relative density evolution of the samples during growth (Fig. 4). The relative density evolution shows that the foams with more catalyst presented a faster decrease in relative density. This observation is in good agreement with the rise times reported in Table 2. Although the samples produced during the DMA tests achieved higher relative densities, the final values are related to those measured on the ex-situ produced samples (Table 3). Foams with higher water dosage (BAF and GBF) always reveal lower densities throughout the whole experiment. However, the effect of the catalyst level is less evident in the DMA samples. A minor decrease in the final density was detected in the large samples when the catalyst level was increased. No appreciable effect was observed for the small samples since slight densification was found with respect to the lower catalyst counterparts. This could be due to the lower curing temperatures or the degasification induced by the constant stress applied to the samples during expansion [20].

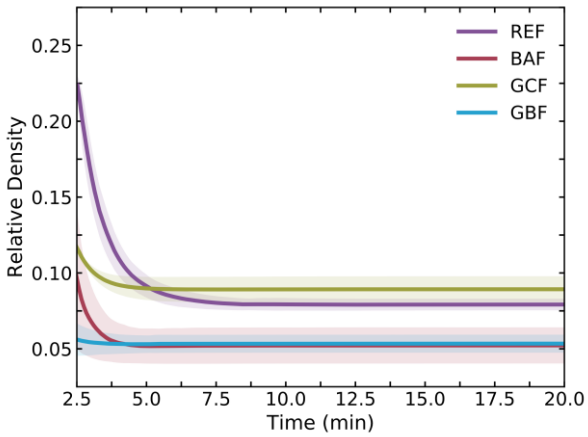

Fig. 4. Relative density evolution with time during 20 minutes from the reaction start for each of the foams in Table 1: REF (0.5 ppw catalyst and 2 ppw water), BAF (0.5 ppw catalyst and 5 ppw water), GCF (1.5 ppw catalyst and 2 ppw water) and GBF (1.5 ppw catalyst and 5 ppw water).

Regarding the standard deviation among repeated runs for the same formulation, the coefficient of variation is significantly lower in the temporal scale than in the absolute values of the modulus. On the one hand, the temporal events that can be detected by means of this technique were well defined in all the experiments. For instance, among repeated experiments for each foam, the coefficient of variation of the vitrification time was found to be below 12% in all cases (Table 4). Additionally, when the curves in Fig. 3 were normalised so that their final modulus is equal to 1, the time at which the foams reach 75% of the last recorded modulus remains fairly constant among repetitions (Table 4). On average, the coefficient of variation for this value is around 20% for these materials. On the other hand, when considering the modulus final values for each of the formulation's subsequent runs, the coefficient of variation was found to be slightly larger.

Regardless of this, conclusions can be drawn from the hierarchy of each sample's final modulus (Fig. 3). Foams with more water content (BAF and GBF) showed lower final modulus values, whereas lower water dosages yielded foams with a higher modulus (REF and GCF). Several factors can account for this phenomenon, such as differences in the cross-linking densities, changes in the polymer matrix's stiffness, or the higher density of the foams with less water. To ensure the accuracy of the final modulus values measured by time-resolved DMA experiments (Fig. 3), the mechanical properties of the cured foams produced in the cup were also measured with DMA. The complex modulus was calculated under the same stress conditions as the time-resolved DMA tests. The obtained values can be compared to the complex moduli measured in-situ (see Table 5). Similar conclusions to those drawn from the *in-situ* results (Fig. 3) can be made from the data summarised in Table 5. The higher the catalyst content, the higher the moduli in comparison to the foams with the same water content. The higher the water content, the lower the modulus with respect to the foams with the same catalyst content. Therefore, a greater amount of water and catalyst in the foam formulation gives rise to materials with lower densities and lower modulus and vice versa. Regarding the absolute values, the cured foams' complex modulus is undoubtedly lower than that of the samples foamed during the time-resolved DMA experiments. This difference can be due to several factors, such as the lower density of the foams produced in a cup, the skin

developed by the samples produced in the mould during in-situ DMA (section 2.2.3) or the different degree of polymerisation attained by the in-situ and ex-situ samples.

Table 5. Complex and Young's modulus obtained from the linear region of the stress-strain curves.

Samples	Catalyst (ppw)	Water (ppw)	Complex modulus after 90 min (MPa)	Complex modulus of the cured foams (MPa)
REF	0.5	2	1.38 ± 0.44	0.54 ± 0.09
BAF	0.5	5	1.05 ± 0.34	0.31 ± 0.03
GCF	1.5	2	1.84 ± 0.33	0.55 ± 0.09
GBF	1.5	5	1.19 ± 0.13	0.30 ± 0.02

Nevertheless, to fully comprehend the changes observed in the samples' viscoelastic properties, it is fundamental to have some information about the reaction kinetics of these systems.

3.4 Reaction kinetics: FTIR Spectroscopy

In order to investigate the temporal evolution of the moduli and its connection to the reactivity of each system, FTIR spectra of the reacting foams were acquired. In this study, two main aspects of the RPU reaction kinetics were monitored: the consumption of isocyanate and the generation of the main products of the gelling and blowing reactions [13,44].

3.4.1 Isocyanate consumption

Fig. 5 depicts the average isocyanate conversion from three experiments with each of the foams in Table 1. None of the foams had fully reacted by the end of the experiment since they reached an isocyanate conversion of around 0.65. Furthermore, the curves of isocyanate conversion for all samples reached around 0.6 in the first 30 minutes of the foam formation, which is equivalent to more than 90% of their final isocyanate conversion. This reveals that the reaction rates are considerably reduced early in the curing process, even if there are still a high number of isocyanate functional groups available to react. Moreover, the speed of isocyanate consumption was calculated for every foam. The time at which the rate of conversion decreases to nearly zero (below 0.025 min^{-1}) varies significantly with the catalyst content. Foams with 1.5 ppw of gelling catalyst (GCF and GBF) reach such speeds after 12 minutes, whereas foams with 0.5 ppw of gelling catalyst (REF and BAF) take more than 25 minutes to experience such a decrease in their reaction

rate. No significant effect was observed when the water content was changed. The speeds of conversion seem to be in good agreement with the vitrification times reported in Table 4, suggesting that after vitrification, the reactions were nearly halted, and the conversion fell to nearly zero [39,45]. Surprisingly, there are no notable differences in the final degree of conversion among foams. Regardless of the concentration of catalyst or water, they all attained conversions close to 0.65. Yet, the different catalysis levels influenced the degree of NCO consumption greatly at short reaction times. Most notably, foams REF and BAF (with 0.5 ppw of catalyst) present lower reaction rates than GCF and GBF with a high catalyst content of 1.5 ppw. Moreover, if samples with the same catalyst content are compared, that with more water has a higher reaction rate.

Concerning the variation between repeated measurements of foams with the same formulation, those with 0.5 ppw of catalyst concentration present higher deviation among experiments (on average, 18% for foam REF and 9% for foam BAF). On the contrary, foams with 1.5 ppw of catalyst reveal lower deviation among repetitions, less than 8% for foam GBF and barely 2% for foam GCF. Therefore, the low catalyst concentration in RPU foams seems to be accountable for a higher degree of dispersion between experiments. This behaviour is in agreement with that observed during the DMA experiments.

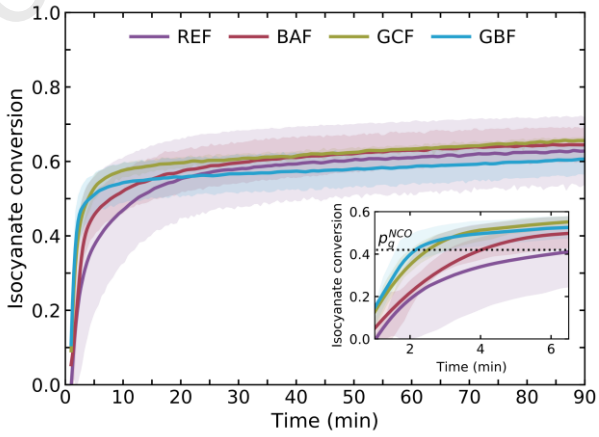

Fig. 5. Average isocyanate conversion versus time for the foams under study: REF (0.5 ppw catalyst and 2 ppw water), BAF (0.5 ppw catalyst and 5 ppw water), GCF (1.5 ppw catalyst and 2 ppw water) and GBF (1.5 ppw catalyst and 5 ppw water).

In addition, the theoretical isocyanate conversion at gel point (p_g^{NCO}) was calculated by means of eqn. 5 as proposed by Macosko and Miller [46]:

$$p_g^{NCO} = \sqrt{\frac{1}{(f-1)\,(g-1)\,r}} \qquad (5)$$

In this equation, *f* and *g* represent the functionalities of the polyol and the isocyanate (reported in Section 2.1.1), respectively. The variable *r* stands for the formulation's stoichiometry ratio (OH/NCO molar ratio), an alternative definition of the isocyanate index (Table 1). This ratio is most commonly used when dealing with PU adhesives or elastomers [47]. Applying this equation, the conversion at the theoretical gel point was found to be 0.427. Thus, it is possible to compare the times at which the foams reach this conversion value (dotted line in the inset of Fig. 5) with the string times measured on the growing foams (Table 2). For foams with high catalyst amount (GCF and GBF), the times at the gelation conversion point are rather short, 2.5 and 2 minutes, respectively. For the foams with low catalyst dosage, the gel conversion time is notably larger, 4 and 6.5 minutes for BAF and REF, respectively. These gel times are in good agreement with the string time reported in Table 2, and only for foam REF, the gel time was slightly longer (6.5 minutes versus 4 minutes).

3.4.2 Products generation

Another key aspect for the characterisation of PU foam formation is the number and rate at which the different reaction products are generated. To gain insight into this, the increasing area of the carbonyl band observed in the ATR-FTIR spectra was analysed by a deconvolution procedure detailed in previous works [6,13,34]. The area under each of the bands corresponding to the blowing and gelling reactions has been added to give the total number of urea and urethane products, respectively.

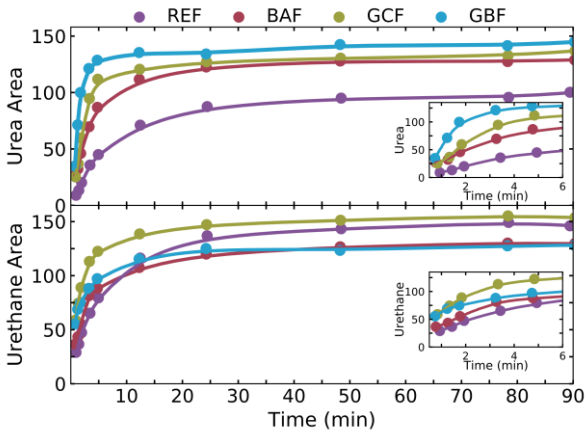

Fig. 6. Total area of urea and urethane products generated with time for the foams under study: REF (0.5 ppw catalyst and 2 ppw water), BAF (0.5 ppw catalyst and 5 ppw water), GCF (1.5 ppw catalyst and 2 ppw water) and GBF (1.5 ppw catalyst and 5 ppw water).

The evolution of the number of urea and urethane products with time and the evolution of the ratio of urethane versus urea products can be seen in Fig. 6 and Fig. 7, respectively. In the first five minutes of reaction, the cross-linking was faster for foams with higher catalyst concentration (GCF and GBF), as proven by the rapid generation of urethane bonds. In addition, these foams suffered a swift increase in their number of urea products, which can be witnessed in the close-ups of Fig. 6. For times longer than 5 minutes after the beginning of the reaction, the urea band's area continued to grow more slowly, suggesting an ongoing gas generation caused by the high reactivity of the water and isocyanate reaction. Yet, from Fig. 4, it is clear that the expansion of foams GBF and GCF halted less than 4 minutes after the reaction started. This time interval coincides with the largest generation of products from both gelling and blowing reactions and the highest isocyanate conversion. Therefore, the faster cross-linking and vitrification of the matrix hampered larger expansions of these samples. Conversely, foams with low catalyst dosage (BAF and most notably REF) underwent a steadier increase in the number of urethane groups. This is in accordance with the isocyanate consumption rates (Fig. 5) and the modulus build-up trends (Fig. 3).

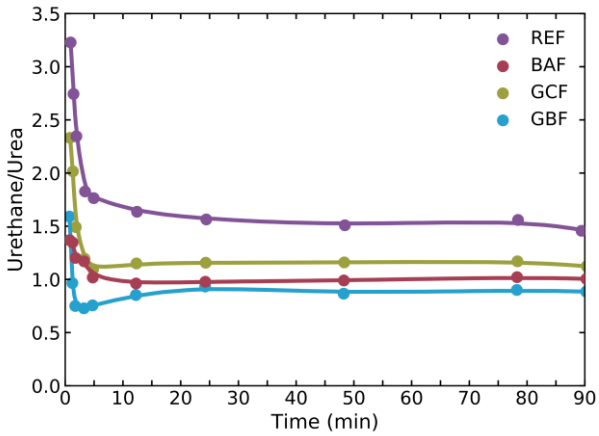

Fig. 7. Ratio of urethane/urea products evolution with time for the foams under study: REF (0.5 ppw catalyst and 2 ppw water), BAF (0.5 ppw catalyst and 5 ppw water), GCF (1.5 ppw catalyst and 2 ppw water) and GBF (1.5 ppw catalyst and 5 ppw water).

However, due to the competitive nature of the blowing and gelling reactions, as polymerisation progressed, the foams with less water content (REF and GCF) were biased towards the generation of urethane bonds surpassing the number of urethane bonds of foams with higher water content. A more linear trend with time can be observed for the urea products. The reference foam (REF) generated fewer urea hard segments. Adding more water to this formulation (BAF) leads to an expected increase in the amount of urea to the detriment of the gelling reaction. Surprisingly, the addition of 1.5 ppw of catalyst in GCF and GBF samples also results in a remarkable increase in the number of ureas with respect to the materials with 0.5 ppw of catalyst (REF and BAF samples) (see Fig. 6). As complementary information to the above, the decrease in the ratio of urethane versus urea (Fig. 7) suggests that the selected catalyst has a dominant role in the blowing reaction.

3.5 Discussion

Moduli evolution of reactive foams can be understood on the basis of the different transformations undergone by the initial raw materials upon reaction, *i.e.* density decrease due to gas generation, development of a stable cellular structure, formation of a highly cross-linked network etc. For the interpretation, we have considered that the results obtained with DMA can be decoupled in two different aspects. On the one hand, the evolution of the moduli as a consequence of the matrix polymerisation and, on the other hand, the final modulus values attained.

First of all, to discard any effect of the density on the modulus values, these have been divided by the squared relative density $\left(E_{foam}/E_{polymer} = (\rho_{foam}/\rho_{solid})^2\right)$.

In such a way, it is possible to observe the impact on the stiffness of the polymer matrix of the different polymer morphologies and reaction products [48,49]. In addition, to obtain a clearer understanding of the relationship between the system's reactivity and the modulus rise, the evolution of the normalised storage modulus, $E_{polymer}$, was plotted against the isocyanate conversion (Fig. 8). Different phenomenological stages can be observed. All materials present an induction stage during which the isocyanate conversion is swift due to the initial components' high reactivity. During this time, the molecular weight is increasing, and the system is being transformed from a rubbery liquid (sol) into a solid network (gel) [38]. Yet, during this first stage, the modulus remains low and practically unchanged since the urethane matrix's cross-linking is still minimal. However, after the gelation conversion point (p_g^{NCO}= 0.427) the modulus of all materials begins to rise. This effect has been reported in previous works for PU thermosets which showed a sudden and steep increase in the complex viscosity after gelation [39]. Notably, during the stage in which the modulus increase is the fastest, the reactivity of the system slows down considerably. Additionally, foams with higher urea content (BAF and GBF, as seen in Fig. 7) show a steeper increase in the polymer's modulus. Last but not least, when the consumption has nearly halted and the reactivity of the system is residual, a slight increase in the modulus is still detected. This increase corresponds to the plateau region of modulus development observed in Fig. 3.

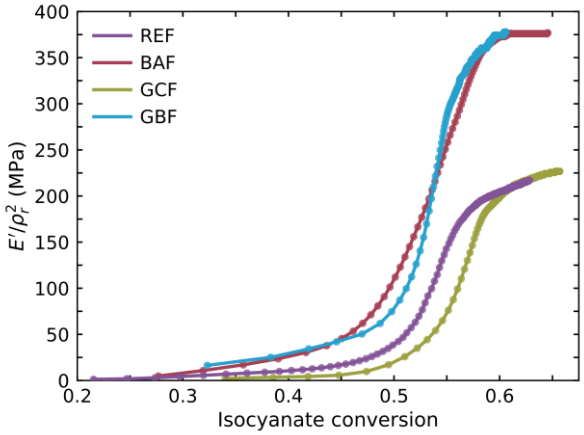

Fig. 8. Evolution of the storage modulus normalised to the relative density as a function of the isocyanate conversion.

Concerning the final modulus values, in Fig. 9, the final foam's complex modulus (Table 5) was normalised to the relative density and is presented against the last value of the normalised complex modulus measured during the *in-situ* experiments.

There is a good correspondence between the properties of the samples produced under compression during the DMA experiments and those of the large-sized foams which underwent a free foaming process (R^2 of the linear fit 0.927). There undoubtedly two groups of foams. The materials with low water content present lower polymer moduli (REF and GCF), whereas those produced with higher water content exhibit higher polymer moduli (BAF and GBF). These results reveal that the modulus trend is similar to that of the ratio of urethane versus urea (Fig. 7), so that the higher the enhancement of the blowing reaction (more urea products), the greater the modulus [50–52]. Furthermore, the addition of water and catalyst (GBF) provides the highest increment in the modulus of the polymer matrix. This increment may be due to the higher number of urea hard segments (Fig. 6), which combined with a good cross-linking, resulted in an increase in the mechanical properties of the polymer matrix. Moreover, these results prove the strong influence of the density on the results reported in Table 5 and Fig. 3.

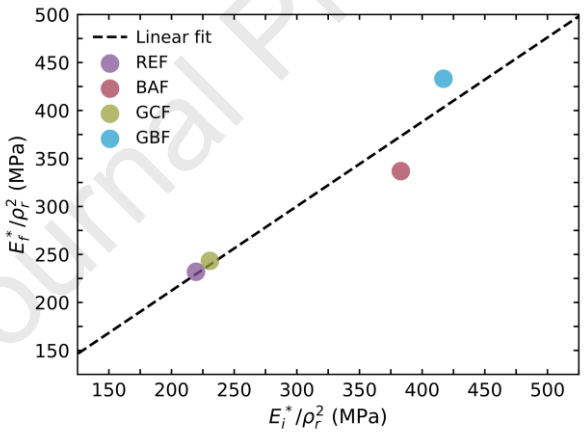

Fig. 9. Normalised Young's modulus of the cured samples (after one week) versus the normalised complex modulus (after 90 minutes) measured *in-situ*.

Throughout this work, the results obtained by means of *in-situ* DMA have been presented in terms of the modulus. Yet, when modelling the evolution of viscoelastic properties and their influence on the generation of a stable cellular structure, the rheological properties are expressed in terms of the polymer viscosity. The DMA modulus values can be converted to viscosity via division by a constant factor (eqn. 6) [28].

$$\eta^* = \frac{G^*}{\omega} = \frac{E^*}{2\,\omega\,(1-\upsilon)} \qquad (6)$$

In eqn. 6, the complex viscosity is connected to the complex modulus through the sample's Poisson's Ratio, υ, and the experiment's radial frequency, ω, which is equal to $2\pi f$ where f is the applied frequency measured in Herz. In our experiments, the frequency was fixed to 1 Hz, and in general, the Poisson's Ratio is low and close to 0.1 for polymeric foams [48]. Therefore, at a constant frequency of 1 Hz, the calculated complex viscosity has the shape of the complex modulus (Fig. 10). Since viscosity increases with the resistance to flow, it is logical that the complex viscosity increases during polymerisation, from low viscosities of around 2000 Pa at the beginning of the polymerisation to practically 50 times the initial value after 90 min of reaction.

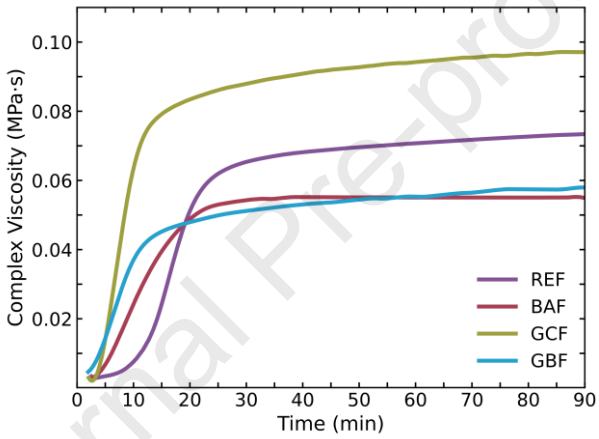

Fig. 10. Complex viscosity as a function of time for each of the foams in Table 1

Likewise, it is possible to divide the complex modulus into two contributions, an in-phase and an out-of-phase component (eqn. 7). The in-phase component, η', is a measure of the energy losses representing the fluid properties of the system and the out-of-phase component, η", is a measure of the energy stored.

$$\eta^* = \eta' - i\eta'' \qquad (7)$$

Therefore, the proposed approach can also be used to determine the complex viscosity and its components, which are key parameters for modelling foam growth and degeneration mechanisms in foaming processes.

4 Conclusions

In this study, the modulus evolution of reactive foams was measured by a newly developed time-resolved DMA method. By means of a customised set-up, it was possible to follow simultaneously the modulus evolution and relative density of reactive foams. The specificity and the reproducibility of the technique were verified by performing repeated experiments on RPU formulations of very different reactivity and final density. From a kinetic point of view, time-resolved DMA's results were verified with ATR-FTIR spectroscopy. Therefore, it was possible to confirm that the foam's polymerisation kinetics had a considerable influence on the dynamics of the modulus development.

Together with these findings and previous rheological models, it was possible to obtain the materials' viscosity development of the materials with time. Classical theories for modelling cell nucleation, cell growth and foam stabilisation phenomena use viscosity-related magnitudes to investigate these mechanisms. Thus, the development of this methodology paves the way for the study of the foaming process of these complex systems.

In short, it has been demonstrated the possibility of obtaining relevant information for the understanding of the foaming process of RPU foams by using a straightforward approach based on time-resolved Dynamic Mechanical Analysis.

Acknowledgements

Financial assistance from the Junta of Castile and Leon (VA202P20) and Spanish Ministry of Science, Innovation and Universities (RTI2018-098749-B-I00) is gratefully acknowledged. Financial support from Junta de Castilla y Leon predoctoral grant of P. Cimavilla-Román, co-financed by the European Social Fund, is also acknowledged.

Data availability statement

The raw/processed data required to reproduce these findings cannot be shared at this time as the data also forms part of an ongoing study.

References

[1] Market data: PlasticsEurope, (n.d.). https://www.plasticseurope.org/en/resources/market-data (accessed January 15, 2021).

[2] N. V. Gama, A. Ferreira, A. Barros-Timmons, Polyurethane foams: Past, present, and future, Materials (Basel). 11 (2018). doi:10.3390/ma11101841.

[3] M. del M. Bernal Ortega, Estudio de nanocompuestos de espumas de poliuretano reforzadas con nanocargas en base carbono, Universidad de Valencia, 2012.

[4] D. Klempner, Handbook of Polymeric Foams and Foam Technology, Hanser Gardner Publications, n.d.

[5] K. Ashida, Polyurethane and Related Foams: Chemistry and Technology, 1st Editio, Taylor & Francis Group, Boca Raton, 2007. doi:10.1128/AAC.03728-14.

[6] M. Santiago-Calvo, Synthesis , Foaming Kinetics and Physical Properties of Cellular Nanocomposites Based on Rigid Polyurethane, Universidad de Valladolid, 2019.

[7] J.O. Akindoyo, M.D.H. Beg, S. Ghazali, M.R. Islam, N. Jeyaratnam, A.R. Yuvaraj, Polyurethane types, synthesis and applications-a review, RSC Adv. 6 (2016) 114453–114482. doi:10.1039/c6ra14525f.

[8] A. Kausar, Polyurethane Composite Foams in High-Performance Applications: A Review, Polym. - Plast. Technol. Eng. 57 (2018) 346–369. doi:10.1080/03602559.2017.1329433.

[9] B. Eling, Ž. Tomović, V. Schädler, Current and Future Trends in Polyurethanes: An Industrial Perspective, Macromol. Chem. Phys. 221 (2020) 1–11. doi:10.1002/macp.202000114.

[10] B. Grignard, J.M. Thomassin, S. Gennen, L. Poussard, L. Bonnaud, J.M. Raquez, P. Dubois, M.P. Tran, C.B. Park, C. Jerome, C. Detrembleur, CO2-blown microcellular non-isocyanate polyurethane (NIPU) foams: From bio- and CO2-sourced monomers to potentially thermal insulating materials, Green Chem. 18 (2016) 2206–2215. doi:10.1039/c5gc02723c.

[11] A. Lee, Y. Deng, Green polyurethane from lignin and soybean oil through non-isocyanate reactions, Eur. Polym. J. 63 (2015) 67–73. doi:10.1016/j.eurpolymj.2014.11.023.

[12] N. V. Gama, B. Soares, C.S.R. Freire, R. Silva, C.P. Neto, A. Barros-Timmons, A. Ferreira, Bio-based polyurethane foams toward applications beyond thermal

insulation, Mater. Des. 76 (2015) 77–85. doi:10.1016/j.matdes.2015.03.032.

[13] M. Santiago-Calvo, J. Tirado-Mediavilla, J.L. Ruiz-Herrero, M.Á. Rodríguez-Pérez, F. Villafañe, The effects of functional nanofillers on the reaction kinetics, microstructure, thermal and mechanical properties of water blown rigid polyurethane foams, Polymer (Guildf). 150 (2018) 138–149. doi:10.1016/j.polymer.2018.07.029.

[14] M. Santiago-Calvo, J. Tirado-Mediavilla, J.L. Ruiz-Herrero, F. Villafañe, M.Á. Rodríguez-Pérez, Long-term thermal conductivity of cyclopentane–water blown rigid polyurethane foams reinforced with different types of fillers, Polym. Int. 68 (2019) 1826–1835. doi:10.1002/pi.5893.

[15] D. V. Pikhurov, A.S. Sakhatskii, V. V. Zuev, Rigid polyurethane foams with infused hydrophilic/hydrophobic nanoparticles: Relationship between cellular structure and physical properties, Eur. Polym. J. 99 (2018) 403–414. doi:10.1016/j.eurpolymj.2017.12.036.

[16] E. Minogue, An in-situ study of the nucleation process of polyurethane rigid foam formation, Dublin City University, 2000.

[17] P. Cimavilla-Román, S. Pérez-Tamarit, M. Santiago-Calvo, M.Á. Rodríguez-Pérez, Influence of silica aerogel particles on the foaming process and cellular structure of rigid polyurethane foams, Eur. Polym. J. 135 (2020) 109884. doi:10.1016/j.eurpolymj.2020.109884.

[18] M.M. Bernal, M.A. Lopez-Manchado, R. Verdejo, In situ foaming evolution of flexible polyurethane foam nanocomposites, Macromol. Chem. Phys. 212 (2011) 971–979. doi:10.1002/macp.201000748.

[19] M.J. Elwell, S. Mortimer, A.J. Ryan, A Synchrotron SAXS Study of Structure Development Kinetics during the Reactive Processing of Flexible Polyurethane Foam, Macromolecules. 27 (1994) 5428–5439. doi:10.1021/ma00097a024.

[20] R. Bouayad, J. Bikard, J.F. Agassant, Compressible flow in a plate/plate rheometer: Application to the experimental determination of reactive expansion's models parameters for polyurethane foam, Int. J. Mater. Form. 2 (2009) 243–260. doi:10.1007/s12289-009-0408-x.

[21] J. Reignier, P. Alcouffe, F. Méchin, F. Fenouillot, The morphology of rigid polyurethane foam matrix and its evolution with time during foaming – New insight by cryogenic scanning electron microscopy, J. Colloid Interface Sci. 552 (2019) 153–165. doi:10.1016/j.jcis.2019.05.032.

[22] R.D. Priester, J. V. Mcclusky, R.E. O'neill, R.B. Turner, M.A. Harthcock, B.L. Davis, FT-IR-A Probe into the Reaction Kinetics and Morphology Development of Urethane Foams, J. Cell. Plast. 26 (1990) 346–367.

doi:10.1177/0021955X9002600405.

[23] M. Kurańska, A. Prociak, S. Michałowski, K. Zawadzińska, The influence of blowing agents type on foaming process and properties of rigid polyurethane foams, Polimery/Polymers. 63 (2018) 672–678. doi:10.14314/polimery.2018.10.2.

[24] M. Santiago-Calvo, S. Pérez-Tamarit, J. Tirado-Mediavilla, F. Villafañe, M.A. Rodríguez-Pérez, Infrared expandometry: A novel methodology to monitor the expansion kinetics of cellular materials produced with exothermic foaming mechanisms, Polym. Test. 66 (2018) 383–393. doi:10.1016/j.polymertesting.2018.02.004.

[25] M. Mar Bernal, S. Pardo-Alonso, E. Solórzano, M.Á. Lopez-Manchado, R. Verdejo, M.Á. Rodriguez-Perez, Effect of carbon nanofillers on flexible polyurethane foaming from a chemical and physical perspective, RSC Adv. 4 (2014) 20761. doi:10.1039/c4ra00116h.

[26] E. Mora, L.D. Artavia, C.W. Macosko, Modulus development during reactive urethane foaming, J. Rheol. (N. Y. N. Y). 35 (1991) 921–940. doi:10.1177/0021955X9102700190.

[27] M.J. Elwell, A.J. Ryan, H.J.M. Gru, H.C. Van Lieshout, H.J.M. Grunbauer, H.C. Van Lieshout, In-situ studies of structure development during the reactive processing of model flexible polyurethane foam systems using FT-IR spectroscopy, synchrotron SAXS and rheology, Am. Chem. Soc. Polym. Prepr. Div. Polym. Chem. 37 (1996) 769–770. doi:10.1021/ma9511208.

[28] K.P. Menard, Dynamic Mechanical Analysis: A Practical Introduction, First Edit, CRC Press, Boca Raton, 2008.

[29] S. Takeda, M. Ohashi, O. Kuwano, M. Kameda, M. Ichihara, Rheological tests of polyurethane foam undergoing vesiculation-deformation-solidification as a magma analogue, J. Volcanol. Geotherm. Res. 393 (2020) 106771. doi:10.1016/j.jvolgeores.2020.106771.

[30] Y. Nawab, S. Shahid, N. Boyard, F. Jacquemin, Chemical shrinkage characterization techniques for thermoset resins and associated composites, J. Mater. Sci. 48 (2013) 5387–5409. doi:10.1007/s10853-013-7333-6.

[31] ASTM D1622-08: Standard Test Method for Apparent Density of Rigid Cellular Plastics, (n.d.).

[32] S. Ebnesajjad, P.R. Khaladkar, Fluoropolymer Applications in the Chemical Processing Industries, Second Edi, Plastics Design Library, 2017.

[33] M.J. Elwell, A.J. Ryan, H.J.M. Grunbauer, H.C. VanLieshout, An FTIR study of reaction kinetics and structure development in model flexible polyurethane

foam systems, Polymer (Guildf). 37 (1996) 1353–1361. doi:10.1016/0032-3861(96)81132-3.

[34] D.P. Queiroz, M.N. De Pinho, C. Dias, ATR-FTIR studies of poly(propylene oxide)/polybutadiene bi-soft segment urethane/urea membranes, Macromolecules. 36 (2003) 4195–4200. doi:10.1021/ma034032t.

[35] A. Marcos-Fernández, A.E. Lozano, L. González, A. Rodríguez, Hydrogen bonding in copoly(ether-urea)s and its relationship with the physical properties, Macromolecules. 30 (1997) 3584–3592. doi:10.1021/ma9619039.

[36] C. Torres-Sánchez, J. Corney, Identification of formation stages in a polymeric foam customised by sonication via electrical resistivity measurements, J. Polym. Res. 16 (2009) 461–470. doi:10.1007/s10965-008-9249-4.

[37] S. Farzaneh, S. Riviere, A. Tcharkhtchi, Rheokinetic of Polyurethane Crosslinking Time-Temperature-Transformation Diagram for Rotational Molding, J. Appl. Polym. Sci. 152 (2012) 2658–2667. doi:10.1002/app.

[38] Z. Yang, H. Peng, W. Wang, T. Liu, Rheological Investigation of Cure Kinetics and Adhesive Strength of Polyurethane Acrylate Adhesive, J. Appl. Polym. Sci. 116 (2010) 2658–2667. doi:10.1002/app.

[39] L.M. Chiacchiarelli, J.M. Kenny, L. Torre, Kinetic and chemorheological modeling of the vitrification effect of highly reactive poly(urethane-isocyanurate) thermosets, Thermochim. Acta. 574 (2013) 88–97. doi:10.1016/j.tca.2013.08.011.

[40] M. Rochery, T.M. Lam, Chemorheology of polyurethane. I. Vitrification and gelation studies, J. Polym. Sci. Part B Polym. Phys. 38 (2000) 544–551. doi:10.1002/(SICI)1099-0488(20000215)38:4<544::AID-POLB6>3.0.CO;2-I.

[41] M. Stanko, M. Stommel, Kinetic prediction of fast curing polyurethane resins by model-free isoconversional methods, Polymers (Basel). 10 (2018). doi:10.3390/polym10070698.

[42] M.T. Aronhime, J.K. Gillham, Time-Temperature-Transformation (Ttt) Cure Diagram of Thermosetting Polymeric Systems., Adv. Polym. Sci. 78 (1986) 83–113. doi:10.1007/BFb0035358.

[43] R. Muller, E. Gérard, P. Dugand, P. Rempp, Y. Gnanou, Rheological Characterization of the Gel Point: A New Interpretation, Macromolecules. 24 (1991) 1321–1326. doi:10.1021/ma00006a017.

[44] J. V. McClusky, R.D. Priester, W.R. Willkomm, M.D. Heaney, M.A. Capel, The use of FT-IR and dynamic saxs to provide an improved understanding of the matrix formation and viscosity build of flexible polyurethane foams, J. Cell.

Plast. 29 (1993) 465. doi:10.1177/0021955X9302900575.

[45] J.K. Fink, Epoxy Resins, in: React. Polym. Fundam. Appl., Plastics Design Library, 2018: pp. 139–223. doi:10.1016/B978-0-12-814509-8.00003-8.

[46] C.W. Macosko, D.R. Miller, A New Derivation of Average Molecular Weights of Nonlinear Polymers, Macromolecules. 9 (1976) 199–206. doi:10.1021/ma60050a003.

[47] S. Oprea, Synthesis and properties of polyurethane elastomers with castor oil as crosslinker, JAOCS, J. Am. Oil Chem. Soc. 87 (2010) 313–320. doi:10.1007/s11746-009-1501-5.

[48] L.J. Gibson, M.F. Ashby, Cellular solids: Structure and Properties, Cambridge: Cambridge Solid State Science Series, Cambridge, 1997.

[49] R.A. Neff, C.W. Macosko, Simultaneous measurement of viscoelastic changes and cell opening during processing of flexible polyurethane foam, Rheol. Acta. 35 (1996) 656–666. doi:10.1007/BF00396514.

[50] A.K. Yusuf, P.A.P. Mamza, A.S. Ahmed, U. Agunwa, Physico-Mechanical Properties of Rigid Polyurethane Foams Synthesized From Modified Castor Oil Polyols, Int. J. Sci. Res. Publ. 6 (2016) 548–556. www.ijsrp.org.

[51] Z. Yang, H. Peng, W. Wang, T. Liu, Crystallization behavior of poly(ε-caprolactone)/layered double hydroxide nanocomposites, J. Appl. Polym. Sci. 116 (2010) 2658–2667. doi:10.1002/app.

[52] W.J. Seo, H.C. Jung, J.C. Hyun, W.N. Kim, Y.B. Lee, K.H. Choe, S.B. Kim, Mechanical, morphological, and thermal properties of rigid polyurethane foams blown by distilled water, J. Appl. Polym. Sci. 90 (2003) 12–21. doi:10.1002/app.12238.

Highlights

- DMA was applied to measure the modulus development of Rigid Polyurethane foams during foaming *in-situ*.
- Employing a customised fixture and using a parallel plate geometry the density evolution was monitored simultaneously during the experiment.
- The modulus build-up profiles recorded with DMA were corroborated by measurements of the reaction kinetics.
- Vitrification times can be inferred from the temporal evolution of the Loss modulus of the foams.

Declaration of interests

☒ The authors declare that they have no known competing financial interests or personal relationships that could have appeared to influence the work reported in this paper.

☐The authors declare the following financial interests/personal relationships which may be considered as potential competing interests: